J Geod
DOI 10.1007/s00190-008-0283-0

ORIGINAL ARTICLE

Triangulated spherical splines for geopotential reconstruction

M. J. Lai · C. K. Shum · V. Baramidze · P. Wenston

Received: 24 January 2008 / Accepted: 28 October 2008

Abstract We present an alternate mathematical technique than contemporary spherical harmonics to approximate the geopotential based on triangulated spherical spline functions, which are smooth piecewise spherical harmonic polynomials over spherical triangulations. The new method is capable of multi-spatial resolution modeling and could thus enhance spatial resolutions for regional gravity field inversion using data from space gravimetry missions such as CHAMP, GRACE or GOCE. First, we propose to use the minimal energy spherical spline interpolation to find a good approximation of the geopotential at the orbital altitude of the satellite. Then we explain how to solve Laplace's equation on the Earth's exterior to compute a spherical spline to approximate the geopotential at the Earth's surface. We propose a domain decomposition technique, which can compute an approximation of the minimal energy spherical spline interpolation on the orbital altitude and a multiple star technique to compute the spherical spline approximation by the collocation method. We prove that the spherical spline constructed by means of the domain decomposition technique converges to the minimal energy spline interpolation. We also prove that the modeled spline geopotential is continuous from the satellite altitude down to the Earth's surface. We have implemented the two computational algorithms and applied them in a numerical experiment using simulated CHAMP geopotential observations computed at satellite altitude (450 km) assuming EGM96 ($n_{\max} = 90$) is the truth model. We then validate our approach by comparing the computed geopotential values using the resulting spherical spline model down to the Earth's surface, with the truth EGM96 values over several study regions. Our numerical evidence demonstrates that the algorithms produce a viable alternative of regional gravity field solution potentially exploiting the full accuracy of data from space gravimetry missions. The major advantage of our method is that it allows us to compute the geopotential over the regions of interest as well as enhancing the spatial resolution commensurable with the characteristics of satellite coverage, which could not be done using a global spherical harmonic representation.

Keywords Geopotential · Spherical splines · Minimal energy interpolation · Domain decomposition technique

The results in this paper are based on the research supported by the National Science Foundation under the grant no. 0327577.

M. J. Lai (✉) · P. Wenston
Department of Mathematics, The University of Georgia, Athens, GA 30602, USA
e-mail: mjlai@math.uga.edu

C. K. Shum
School of Earth Sciences, Ohio State University, Columbus, OH 43210, USA

V. Baramidze
Department of Mathematics, Western Illinois University, Macomb, IL 61455, USA

1 Introduction

Advances in the measurement of the gravity have with modern free-fall methods have reached accuracies of 10^{-9} g ($1\,\mu$Gal or $10\,\mathrm{nm/s}^2$), allowing the observations of mass transports within the Earth's interior to be measured a commensurate accuracy, and surface height change (Forsberg et al. 2005). As a result and during this Decade of the Geopotential, satellite missions launched to exploit the gravity measurement accuracy include the challenging minisatellite payload (CHAMP) (Reigber et al. 2004), the gravity recovery and climate experiment (GRACE) (Tapley et al. 2004) gravimetry missions, and the Gravity field and steady-state ocean circulation explorer (GOCE) satellite gradiometry mission (to be launched October 2008) (Rummel et al. 1999). These satellite missions provide global synoptic mapping of geodynamic processes and climate-sensitive mass transports within the Earth, providing a tool to study Earth sciences including climate change.

The geopotential function V is defined on $\mathbf{R}^3$ such that the gradient ∇V is the gravitational field. Traditionally, V is reconstructed by using spherical harmonic functions (cf., e.g., Tapley et al. 2004 to model data from the GRACE mission). Recently, several new methods have been proposed. Spherical wavelet methods were studied in Freeden et al. (1998, 2002) and results were surveyed in Freeden et al. (2003), Freeden and Schreiner (2005), and Fengler et al. (2007). Other spherical wavelet techniques include Poisson multipole wavelets (cf. Chambodut et al. 2005), wavelet frames (cf. Panet et al. 2005, 2006) and Blackman spherical wavelets (cf. Schmidt et al. 2005a,b,c).

Other techniques have been developed and they are distinct from the classical gravity field inversion approach (cf. Lehmann and Klees 1999) and resulted in global spherical harmonic geopotential monthly solutions using GRACE data (Tapley et al. 2004). These techniques include the processing of GRACE intersatellite range-rate data using the Fredholm integral approach (Mayer-Gürr et al. 2006), the mass concentrations (mascon) approach (Rowlands et al. 2005), and the energy conservation approach to compute satellite in situ geopotential (CHAMP) or the disturbance potential (GRACE) data (Han et al. 2006). The second step of some of the above mentioned techniques, for example, used a regional inversion approach with stochastic least squares collocation and 2D-FFT which achieved enhanced spatial resolution than that of solutions based on global spherical harmonics (Han et al. 2003). Spherical splines were considered as a technique for geodetic inverse problem in Schneider (1996). Several spline functions including triangulated spherical splines were suggested for the forward modeling of the geopotential (Jekeli 2005).

In this paper, we propose to use triangulated spherical splines to compute an approximation of the geopotential. The triangulated spherical splines over the unit sphere $\mathbb{S}^2$ were introduced and studied by Alfeld, Neamtu and Schumaker in a series of three papers (Alfeld et al. 1996a,b,c). These spline functions are smooth piecewise spherical harmonic polynomials over triangulation of the unit spherical surface $\mathbb{S}^2$. Basic properties of triangulated spherical splines are summarized in Lai and Schumaker (2007). They can have locally supported basis functions, which are completely different from the spherical splines defined in Freeden et al. (1998). A straightforward computational method to use these triangulated spherical splines for scattered data fitting and interpolation is given in our earlier paper (Baramidze et al. 2006). We explain how to use triangulated spherical splines directly without constructing locally supported basis functions like finite elements for constructing fitting and/or interpolating spherical spline functions from any given data locations and values. In this direct method, we explain how to use an iterative method to solve some constraint minimization problems with smoothness conditions and interpolation conditions as constraints. In addition, the approximation property of minimal energy spherical spline interpolation can be found in Baramidze (2005). The approximation property implies that the triangulated spherical spline interpolation by using the minimal energy method gives an excellent approximation of sufficiently smooth functions over the surface of the unit sphere. However, when using the minimal energy method to find spherical spline interpolation of the geopotential, the matrix associated with the method is relatively large for the given large amount of the data from a spaceborne gravimetry satellite. In this paper we propose a new computational method called a domain decomposition technique to compute an approximation of the global minimal energy spline interpolation. This technique is a generalization of the same technique in the planar setting (cf. Lai and Schumaker 2008). It enables us to do the computation in parallel and hence, effectively reduce the computational time.

In this study, we choose, in a demonstration study, to use the simulated satellite data of in situ geopotential measurements (in $\mathrm{m}^2/\mathrm{s}^2$) which was computed for the gravity mission satellite, The CHAllenging Minisatellite Payload (CHAMP) (cf. Reigber et al. 2004). CHAMP is a German geodetic satellite, launched on July 15, 2000, with a circular orbit at an altitude of 450 km and orbital inclination of 87°. In Figs. 1 and 2, we show a set of CHAMP potential data coverage for a 2-day period (two methods for these data locations are shown to illustrate the fact that seemingly equally distributed measurement locations shown in Fig. 1 are corresponding to scattered locations in Fig. 2 which indicates that it is hard to find an interpolation using a tensor product of two trigonometric polynomials. In this study, we used a truncated (at $n_{\max} = 90$) EGM96 geopotential model to generate simulated geopotential measurements (with noise at $1\,\mathrm{m}^2/\mathrm{s}^2$) at the CHAMP orbital altitude (450 km) over a time period of 30 days. The total amount of simulated data is 86,400 (2,880 measurements per day for 30 days). We intend to demonstrate the validity of the spherical spline modeling using the CHAMP geopotential measurements (at the orbital altitude), and using the resulting spherical spline modeled gravity field to predict (and compare with) the "truth" geopotential values (computed using EGM96, $n_{\max} = 90$) at the Earth's surface.

Since the purpose of the research to reconstructing the geopotential is to find a good approximation of the geopotential values on the Earth's surface, we use the above approximation of the geopotential on the satellite orbit to approximate the geopotential on the Earth's surface. To this end, we recall the classic theory of geopotential (cf., e.g.,

Journal: 190 MS: 283 CMS: GIVE CMS ☐ TYPESET ☐ DISK ☐ LE ☐ CP Disp.:2008/11/10 Pages: 14 Layout: Large

Fig. 1 Geopotential data locations

Heiskanen and Moritz 1967). The geopotential function V defined on the $\mathbf{R}^3$ space outside of the Earth satisfies the Laplace's equation with Dirichlet boundary condition on the Earth's surface. If the boundary values $V(u)$ or $V(R_e, \theta, \lambda)$ are known for all $u = (x, y, z)$ over the surface of the imaginary sphere with mean Earth's radius $R_e = 6,371.138\,\text{km}$ with $x = R_e \sin\theta \cos\lambda$, $y = R_e \sin\theta \sin\lambda$, and $z = R_e \cos\theta$, the solution of Laplace's equation outside the sphere can be explicitly given in terms of spherical harmonics or in terms of Poisson integral. That is, the solution V to the exterior problem ($|u| = \sqrt{x^2 + y^2 + z^2} > R_e$) can be represented in terms of an infinite sum:

$$V(u) = \sum_{n=0}^{\infty} \left(\frac{R_e}{|u|}\right)^n Y_n(\theta, \lambda), \tag{1.1}$$

where

$$Y_n(\theta, \lambda) = \frac{2n+1}{4\pi} \int\limits_{\lambda'=0}^{2\pi} \int\limits_{\theta'=0}^{\pi} V(R_e, \theta', \lambda') P_n(\cos\psi) \times \sin\theta' \mathrm{d}\theta' \mathrm{d}\lambda' \tag{1.2}$$

are spherical harmonics, P_n are Legendre polynomials, and

$$\cos\psi = \cos\theta \cos\theta' + \sin\theta \sin\theta' \cos(\lambda - \lambda').$$

It is known that when $|u| = R_e$, the series in (1.1) does not converge uniformly and thus one does not know how many terms on the right-hand side needed to approximate $V(u)$ for any fixed point u.

In addition to (1.1), we also know Poisson integral representation of the solution V for $|u| > R_e$, i.e.,

$$V(u) = R_e \frac{|u|^2 - R_e^2}{4\pi} \int\limits_{\lambda'=0}^{2\pi} \int\limits_{\theta'=0}^{\pi} \frac{V(R_e, \theta', \lambda')}{\ell^3} \sin\theta' \mathrm{d}\theta' \mathrm{d}\lambda', \tag{1.3}$$

where $\ell = \sqrt{|u|^2 - 2|u| R_e \cos\psi + R_e^2}$ is the distance from u to v with $|v| = R_e$ and angles θ', λ'.

It is known that the geopotential V is infinitely differentiable. By the approximation property of the minimal energy spline interpolation (cf. Baramidze 2005) based on the approximation properties of spherical spline functions (cf. Neamtu and Schumaker 2004), the spherical interpolatory spline S_V of the geopotential measurement data at the in situ orbital surface at $R_o := R_e + 450\,\text{km}$ altitude is a very good approximation of the geopotential V (see Sect. 2). Intuitively, we may replace V by S_V in (1.3). That is,

$$S_V(u) \approx R_e \frac{|u|^2 - R_e^2}{4\pi} \int\limits_{\lambda'=0}^{2\pi} \int\limits_{\theta'=0}^{\pi} \frac{V(R_e, \theta', \lambda')}{\ell^3} \sin\theta' \mathrm{d}\theta' \mathrm{d}\lambda', \tag{1.4}$$

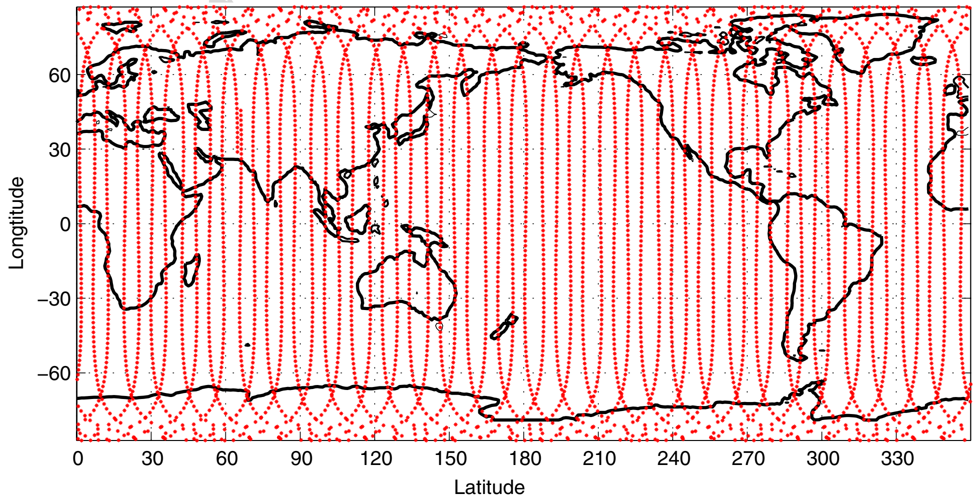

Fig. 2 Planar view of geopotential data locations

Journal: **190** MS: **283** CMS: **GIVE CMS** ☐TYPESET ☐DISK ☐LE ☐CP Disp.:**2008/11/10** Pages: **14** Layout: **Large**

where $\approx$ means that $S_V(u) = V(u)$ at measurement locations and $S_V(u)$ is very closed to $V(u)$ at other locations.

Next we approximate V on the surface of the Earth in the above formula by using triangulated spherical splines. Let $S_d^0(\triangle_e)$ be the space of all continuous spherical splines of degree d over $\triangle_e$ which is induced by the underlying triangulation $\triangle$ of S_V. We find $s_V \in S_d^0(\triangle_e)$ solving the following collocation method:

$$S_V(u) = R_e \frac{|u|^2 - R_e^2}{4\pi} \int\limits_{\lambda'=0}^{2\pi} \int\limits_{\theta'=0}^{\pi} \frac{s_V(R_e, \theta', \lambda')}{\ell^3} \sin\theta' \mathrm{d}\theta' \mathrm{d}\lambda', \tag{1.5}$$

for $u \in \mathcal{D}_\triangle^d$, where $\mathcal{D}_\triangle^d$ is a set of domain points on the orbital surface (to be precise later). The reason we use $S_d^0(\triangle_e)$ is that the geopotential on the surface of the Earth may not be a very smooth function. It should be approximated by spherical splines in $S_d^0(\triangle_e)$ better than by spline functions in $S_d^r(\triangle_e)$ with $r \geq 1$. We need to show that the linear system (1.5) above is invertible for certain triangulations. Then we continue to prove that s_V yields an approximation of the geopotential V on the Earth's surface (see Sect. 4). To compute s_V, we shall use a so-called multiple star technique so that the computation can be done in parallel. In Sect. 4 we shall explain this technique and show that the numerical solution from the multiple star technique converges.

The above discussions outline a theoretical basis for approximating geopotential at any point on the surface $R_e\mathbb{S}^2$ by using triangulated spherical splines. Our triangulated spherical spline approach is certainly different from the traditional and classic approach by spherical harmonic polynomials. For example, in Han et al. (2002), a least squares method is used to determine the coefficients in the spherical harmonic expansion up to degree $n = 70$ to fit the CHAMP measurements. The total number of coefficients is $70 \times 71/2 = 4,970$. The rigorous estimation of these coefficients potentially requires many hours of CPU time of a supercomputer back to 10 years ago. When evaluating the geopotential at any point, all these 4,970 terms have to be evaluated since each harmonic basis function Y_n is globally supported over the sphere. This requires a lot of computation time. As the degree n of spherical harmonics increases, spherical harmonic polynomials Y_n oscillate more and more frequently and the evaluation of Y_n with large degree n is very sensitive to the accuracy of the locations.

The advantages of triangulated spherical splines over the method of spherical harmonic polynomials are as follows:

(1) Our spherical spline solution is an interpolation of the given geopotential data measurements instead of a least squares data fitting. Due to computer capacity, we are not able to interpolate the data values within the machine epsilon. In our computation, the root mean square error over these 86,400 values is 0.018 $\mathrm{m}^2/\mathrm{s}^2$ while the least square fit has the root mean square value about 0.5 $\mathrm{m}^2/\mathrm{s}^2$.

(2) Our solution is solved in parallel in the sense that the solution is divided into many small blocks and each small block is solved independently while in the least squares method, the observation matrix is dense and of large size and hence, is relatively expensive to solve;

(3) Our solution can be efficiently evaluated at any point since only a few terms which maybe nonzero at the point. For example, for a spherical spline of degree $d = 5$, there are only 21 terms of spherical Bernstein Bézier polynomials (cf. 2.2 in the next section) which are nonzero over the triangle where a point of interest locates. However, for a spherical harmonic expansion, there are about n^2 terms of the Legendre polynomials. The their calculation require a lot of computation time.

(4) Our algorithms allow us to compute an approximation of the geopotential over any region ω on the Earth's surface directly from the measurements of a satellite on the orbital level. That is, to compute s_V over $\omega \subset R_e\mathbb{S}^2$, we need $S_V(u)$ for $u \in \Omega$ on $R_o\mathbb{S}^2$ (see Sect. 4). Note that Ω is corresponding to an enlarged region on $R_e\mathbb{S}^2$ covering ω. To compute S_V over Ω on the orbital surface, we use the measurements from a satellite over a larger region $\mathrm{star}^q(\Omega)$ (see Sect. 3).

Let us summarize our approach as follows: First we compute a spherical spline interpolation S_V of geopotential values at these 86, 400 data locations over the orbital surface by using the minimal energy method. Since computing a minimal energy interpolant for such a large data set requires a significant memory storage and high speed computer resources, we shall use a domain decomposition technique to overcome this difficulty. We shall explain the technique and computation in Sect. 3. Secondly we shall solve (1.5) to find a spherical spline approximation s_V on the surface of the Earth. We begin with showing that s_V is a good approximation of V and then discuss how to compute s_V by using a multiple star technique (another version of our domain decomposition technique). All these will be given in Sect. 4. Finally in Sect. 5 we conclude that our triangular spherical splines are effective and efficient for computing the geopotential on the Earth's surface.

2 Preliminaries

2.1 Spherical spline spaces

Given a set $\mathcal{P}$ of points on the sphere of radius 1, we can form a triangulation $\triangle$ using the points in $\mathcal{P}$ as the vertices of $\triangle$ by using the Delaunay triangulation method. Alternatively,

Journal: 190 MS: 283 CMS: GIVE CMS ☐ TYPESET ☐ DISK ☐ LE ☐ CP Disp.:2008/11/10 Pages: 14 Layout: Large

Fig. 3 A uniform triangulation of the sphere

we can use eight similar spherical triangles to partition the unit sphere $\mathbb{S}^2$ and denote the collection of triangles by $\triangle_0$. Then we uniformly refine $\triangle_0$ by connecting the midpoints of three edges of each triangle in $\triangle_0$ to get a new refined triangulation $\triangle_1$. Then we repeat the uniform refinement to get $\triangle_2, \triangle_3, \ldots$. See Fig. 3 for a uniform triangulation over a surface of the Earth. In this paper, we will assume that the triangulation $\triangle$ is regular in the sense that: (1) any two triangles do not intersect each other or share either a common vertex or a common edge; (2) every edge of $\triangle$ is shared by exactly two triangles.

Let

$$S_d^r(\Delta) = \{s \in C^r(\mathbb{S}^2), s|_\tau \in \mathcal{H}_d, \tau \in \Delta\}$$

be the space of homogeneous spherical splines of degree d and smoothness r over Δ. Here $\mathcal{H}_d$ denotes the space of spherical homogeneous polynomials of degree d (cf. Alfeld et al. 1996a). This spline space can be easily used for interpolation and approximation on sphere if any spline function in $S_d^r(\Delta)$ is expressed in terms of spherical Bernstein Beziér polynomials and the computational methods in Baramidze et al. (2006) are adopted.

To be more precise, we write each spline function $s \in S_d^r(\Delta)$ by

$$s = \sum_{T\in\Delta} \sum_{i+j+k=d} c_{ijk}^T B_{ijk}^T, \qquad (2.1)$$

where B_{ijk}^T is called spherical Bernstein basis function which is only supported on triangle T and c_{ijk}^T are coefficients associated with B_{ijk}^T. More precisely, let $T = \langle v_1, v_2, v_3\rangle$ be a spherical triangle on the unit sphere with nonzero area. Let $b_1(v),\ b_2(v),\ b_3(v)$ be the trihedral barycentric coordinates of a point $v \in \mathbf{S}^2$ satisfying

$$v = b_1(v)v_1 + b_2(v)v_2 + b_3(v)v_3.$$

We note that the linear independence of the vectors $v_1,\ v_2$ and $v_3 \in \mathbf{R}^3$ imply that $b_1(v)$, $b_2(v)$, and $b_3(v)$ are uniquely determined. Clearly, $b_1(v)$, $b_2(v)$, and $b_3(v)$ are linear functions of v. It was shown in Alfeld et al. (1996a) that the set

$$B_{ijk}^T(v) = \frac{d!}{i!j!k!} b_1(v)^i b_2(v)^j b_3(v)^k, \quad i+j+k=d \qquad (2.2)$$

of spherical Bernstein-Bézier (SBB) basis polynomials of degree d forms a basis for $\mathcal{H}_d$ restricted to the unit spherical surface $\mathbf{S}^2$. Note that when $d = 5$, there are 21 basis polynomials B_{ijk}^T, $i + j + k = 5$. More about spherical splines can be found in Lai and Schumaker (2007).

2.2 Minimal energy spline interpolations

Next we briefly explain one of the computational methods presented in Baramidze et al. (2006). Suppose we are given values $\{f(v), v \in \mathcal{P}\}$ of an unknown function f on a set $\mathcal{P}$. Let

$$U_f := \{s \in S_d^r(\Delta) : s(v) = f(v), v \in \mathcal{P}\}$$

be the set of all splines in $\mathcal{S} \subseteq S_d^r(\triangle)$ that interpolate f at the points of $\mathcal{P}$. Then a commonly used way (cf. Freeden and Schreiner 1998) to create an approximation of f is to choose a spline $S_f \in U_f$ such that

$$\mathcal{E}_\delta(S_f) = \min_{s\in U_f} \mathcal{E}_\delta(s), \qquad (2.3)$$

where $\mathcal{E}_\delta$ is an energy functional:

$$\mathcal{E}_\delta(f) = \int_{\mathbb{S}^2} \left(\left|\frac{\partial^2}{\partial x^2} f_\delta\right|^2 + \left|\frac{\partial^2}{\partial y^2} f_\delta\right|^2 + \left|\frac{\partial^2}{\partial z^2} f_\delta\right|^2 + \left|\frac{\partial^2}{\partial x \partial y} f_\delta\right|^2 + \left|\frac{\partial^2}{\partial x \partial z} f_\delta\right|^2 + \left|\frac{\partial^2}{\partial y \partial z} f_\delta\right|^2 \right) \mathrm{d}\theta \mathrm{d}\phi, \qquad (2.4)$$

where, since f is defined only on $\mathbb{S}^2$, we first extend f into a function f_δ defined on $\mathbf{R}^3$ to take all partial derivatives and then restrict them on the unit spherical surface $\mathbb{S}^2$ for integration. Here, we use $\mathcal{E}_\delta$ for $\delta = 0$ or $\delta = 1$ to denote the even and odd homogeneous extensions of f. In the rest of the paper, we should fix $\delta = 1$.

We refer to S_f in Eq. (2.3) the (global) minimal energy interpolating spline. To compute S_f, we use the coefficient vector $\mathbf{c}$ consisting of $c_{ijk}^T, i + j + k = d, T \in \triangle$ (see 2.1) to represent each spline function $s \in S_d^{-1}(\triangle)$, where $S_d^{-1}(\triangle)$ denotes the space of piecewise spherical polynomials of degree d over triangulation $\triangle$ without any

Journal: 190 MS: 283 CMS: GIVE CMS ☐TYPESET ☐DISK ☐LE ☐CP Disp.:2008/11/10 Pages: 14 Layout: Large

smoothness. To ensure the C^r continuity across each edge of $\triangle$, we impose the smoothness conditions over every edge of $\triangle$. Let M denote the smoothness matrix such that

$$M\mathbf{c} = 0$$

if and only if $s \in S_d^r(\triangle)$. Note that we can assemble interpolation conditions into a matrix K, according to the order in which the coefficient vector $\mathbf{c}$ is organized. Then $K\mathbf{c} = \mathbf{F}$ is the linear system of equations such that the coefficient vector $\mathbf{c}$ of a spline s interpolates f at the data sites $\mathcal{P}$.

The problem of minimizing (2.3) over $S_d^r(\triangle)$ can be formulated as follows (cf. Baramidze et al. 2006):

$$\text{minimize } \mathcal{E}_\delta(s), \text{ subject to } M\mathbf{c} = 0 \quad \text{and} \quad K\mathbf{c} = \mathbf{F}.$$

To simplify the data management we linearize the triple indices of SBB-coefficients c_{ijk} as well as the indices of the basis functions B_{ijk}^d. By using the Lagrange multipliers method, we solve the following linear system

$$\begin{bmatrix} E & K' & M' \\ K & 0 & 0 \\ M & 0 & 0 \end{bmatrix} \begin{bmatrix} c \\ \eta \\ \gamma \end{bmatrix} = \begin{bmatrix} 0 \\ \mathbf{F} \\ 0 \end{bmatrix}. \tag{2.5}$$

Here γ and η are vectors of Lagrange multipliers, K' and M' denotes the transposes of K and M, respectively, and the energy matrix E is defined as follows. E = diag $(E_T,$ $T \in \triangle)$ is a diagonally block matrix. Each block $E_T = (e_{mn})_{1 \le m,n \le d(d+1)/2}$ is associated with a triangle $T \in \triangle$ and contains the following entries

$$e_{mn} := \int_T (\diamond B_m^T(v)) \cdot \diamond(B_n^T(v)) d\sigma(v), \tag{2.6}$$

where B_m and B_n denote SBB polynomial basis functions B_{ijk}^T of degree d corresponding to the order of the linearized triple indices (i, j, k), $i + j + k = d$. Here, $\diamond$ denotes the second order derivative vector, i.e.,

$$\diamond f = \left(\frac{\partial^2}{\partial x^2} f, \frac{\partial^2}{\partial y^2} f, \frac{\partial^2}{\partial z^2} f, \frac{\partial^2}{\partial x \partial y} f, \frac{\partial^2}{\partial x \partial z} f, \frac{\partial^2}{\partial y \partial z} f\right) \tag{2.7}$$

and $\cdot$ denotes the dot product of two vectors in Eq. (2.6).

Note that E is a singular matrix. The special linear system is now solved by using the iterative method: Writing the above singular linear system Eq. (2.5) in the following form

$$\begin{bmatrix} A & L' \\ L & 0 \end{bmatrix} \begin{bmatrix} \mathbf{c} \\ \lambda \end{bmatrix} = \begin{bmatrix} F \\ G \end{bmatrix},$$

where $A = E$ and $L = [K; M]$ are appropriate matrices. The system can be successfully solved by using the following iterative method (cf. Awanou and Lai 2005)

$$\begin{bmatrix} A & L' \\ L & -\epsilon I \end{bmatrix} \begin{bmatrix} \mathbf{c}^{(\ell+1)} \\ \lambda^{(\ell+1)} \end{bmatrix} = \begin{bmatrix} F \\ G - \epsilon\lambda^{(\ell)} \end{bmatrix},$$

for $l = 0, 1, 2, \ldots$, where $\epsilon > 0$ is a fixed number, e.g., $\epsilon = 10^{-4}$, $\lambda^{(\ell)}$ is iterative solution of a Lagrange multiplier with $\lambda^0 = 0$ and I is the identity matrix. The above matrix iterative steps can in fact be rewritten as follows:

$$\left(A + \frac{1}{\epsilon} L'L\right) \mathbf{c}^{(l+1)} = AF\mathbf{c}^{(l)} + \frac{1}{\epsilon} L'G$$

with $\mathbf{c}^{(0)} = 0$. It is known that under the assumption that A is symmetric and positive definite with respect to L, the vectors $c^{(\ell)}$ converge to the solution $\mathbf{c}$ in the following sense: there exists a constant C such that

$$\|\mathbf{c}^{(k+1)} - \mathbf{c}\| \le C\epsilon \|\mathbf{c}^{(k)} - \mathbf{c}\|$$

for all k (cf. Awanou and Lai 2005). Since A may be of large size, we shall introduce a new technique to make the computational method more affordable in the next section.

The approximation properties of minimal energy interpolating spherical splines are studied in (cf. Baramidze 2005). Let us state here briefly that for the homogeneous spherical splines of degree d under certain assumptions on triangulation $\triangle$ we have

$$\|S_f - f\|_{\infty,\mathbb{S}^2} \le C|\triangle|^2 |f|_{2,\infty,\mathbb{S}^2}$$

for $f \in C^2(\mathbb{S}^2)$ and d odd, and

$$\|S_f - f\|_{\infty,\mathbb{S}^2} \le C'|\triangle|^2 |f|_{2,\infty,\mathbb{S}^2} + C''|\triangle|^3 |f|_{3,\infty,\mathbb{S}^2}$$

for $f \in C^3(\mathbb{S}^2)$ and d even, where $|f|_{2,\infty,\mathbb{S}^2}$ stands for the maximum norm of all second order derivatives of f over the sphere $\mathbb{S}^2$ (cf. Neamtu and Schumaker 2004) and similar for $|f|_{3,\infty,\mathbb{S}^2}$ which is the maximum norm of all third order derivatives of f over $\mathbb{S}^2$. Here $|\triangle|$ denotes the size of triangulation, i.e., the largest diameter of the spherical cap containing triangle T for $T \in \triangle$. Since geopotential V is the solution of Laplace's equation, it is infinitely many differentiable. It follows that S_V approximates V very well as long as $|\triangle|$ goes to zero.

3 Approximation of geopotential over the orbital surface

3.1 Explanation of the domain decomposition technique

Since the given simulated set of in situ geopotential measurements collected by CHAMP during 30 days amounts to 86,400 locations and values, computing a minimal energy interpolant for such a large set requires a significant amount of computer memory storage and high speed computer resources. To overcome this difficulty, we use a domain decomposition technique which will be used to approximate the minimal energy spline interpolant.

The domain decomposition method can be explained as follows. Divide the spherical domain $\mathbb{S}^2$ into several smaller non-overlapping subdomains Ω_i, $i = 1, \ldots, n$ along the

Journal: 190 MS: 283 CMS: GIVE CMS ☐ TYPESET ☐ DISK ☐ LE ☐ CP Disp.:2008/11/10 Pages: 14 Layout: Large

edges of existing triangulation $\triangle$ of Ω. For example, we may choose each triangle of $\triangle$ is a subdomain. Fix $q \geq 1$. Let $\mathrm{star}^q(\Omega_i)$ be a q-star of subdomain Ω_i which is defined recursively by letting $\mathrm{star}^0(\Omega_i) = \Omega_i$ and

$$\mathrm{star}^q(\Omega_i) := \cup\{T \in \triangle, T \cap \mathrm{star}^{q-1}(\Omega_i) \neq \emptyset\} \tag{3.1}$$

for positive integers $q = 1, 2, \ldots$.

Instead of solving the minimal energy interpolation problem over the entire spherical surface, we solve the minimal energy spherical spline interpolation problem over each q-star domain $\mathrm{star}^q(\Omega_i)$ by using the spherical spline space $\mathcal{S}_{i,q} := S_d^r(\mathrm{star}^q(\Omega_i))$ for $i = 1, 2, \ldots, n$. Let $s_{f,i,q}$ be the minimal energy solution over $\mathrm{star}^q(\Omega_i)$. That is, let

$$U_{f,i,q} := \{s \in \mathcal{S}_{i,q}, s(v) = f(v), \forall v \in \mathrm{star}^q(\Omega_i) \cap \mathcal{P}\}.$$

Then $s_{f,i,q} \in U_{f,i,q}$ is the spline satisfying

$$\mathcal{E}_{i,q}(s_{f,i,q}) = \min\{\mathcal{E}_{i,q}(s), s \in U_{f,i,q}\}, \tag{3.2}$$

where

$$\mathcal{E}_{i,q}(s) := \sum_{T \in \mathrm{star}^q(\Omega_i)} \int_T \diamond(s) \cdot \diamond(s) \mathrm{d}\sigma \tag{3.3}$$

with $\diamond$ being defined in (2.7). It can be shown that $s_{f,i,q}|_{\Omega_i}$ approximates the global minimal energy spline (2.3) $S_f|_{\Omega_i}$ very well. That is, we have

Theorem 3.1 *Suppose we are given data values $f(v)$ over scattered data locations $v \in \mathcal{P}$ for a sufficiently smooth function f over the unit sphere. Let S_f be the minimal energy interpolating spline satisfying (2.3). Let $s_{f,i,k}$ be the minimal energy interpolating spline over $\mathrm{star}^q(\Omega_i)$ satisfying (3.2). Then there exists a constant $\sigma \in (0, 1)$ such that for $q \geq 1$*

$$\begin{aligned} ||S_f - s_{f,i,q}||_{\infty,\Omega_i} &\leq C_0 \sigma^q \left(\tan \frac{|\triangle|}{2}\right)^2 \\ &\times (C_1 |f|_{2,\infty,\mathbb{S}^2} + C_2 ||f||_{\infty,\mathbb{S}^2}), \end{aligned} \tag{3.4}$$

if $f \in C^2(\mathbb{S}^2)$ and d is odd. Here C_0, C_1 and C_2 are constants depending on d and $\beta = |\triangle|/\rho_\triangle$, where $\rho_\triangle$ denotes the smallest radius of the inscribed caps of all triangles in $\triangle$. If $f \in C^3(\mathbb{S}^2)$ and d is even

$$\begin{aligned} ||S_f - s_{f,i,q}||_{\infty,\Omega_i} &\leq C_0 \sigma^q \left(\tan \frac{|\triangle|}{2}\right)^2 \\ &\times (C_3 |f|_{2,\infty,\mathbb{S}^2} + C_4 |f|_{3,\infty,\mathbb{S}^2} + C_3 ||f||_{\infty,\mathbb{S}^2}), \end{aligned} \tag{3.5}$$

for positive constants C_4 and C_5 depending on d and β.

One significant advantage of the domain decomposition technique is that $s_{f,i,q}$ can be computed over subdomain $\mathrm{star}^q(\Omega_i)$ independent of $s_{f,j,q}$ for $j \neq i$. Thus, the computation can be done in parallel. Usually, we choose each triangle in $\triangle$ as a subdomain. We use $s_{f,i,q}$ to approximate S_f over Ω_i. The collection of $s_{f,i,q}|_{\Omega_i}$ is a very good approximation of S_f over Ω. If the computation for each subdomain requires a reasonable time, so is the approximation of the global solution.

The proof of Theorem 3.1 is quite technique in mathematics. We omit the detail here. For the interested reader (see Baramidze 2005; Lai and Schumaker 2008). In the following subsection we present some numerical experiments to demonstrate the convergence of local minimal energy interpolatory splines to the global one.

3.2 Computational results on the orbital surface

We have implemented our domain decomposition technique for the reconstruction of geopotential over the orbital surface in both MATLAB and FORTRAN. To make sure that our computational algorithms work correctly, we first choose several spherical harmonic functions to test and verify the accuracy of the computational algorithm. Then we apply our algorithm to the CHAMP simulated data set (geopotential observations computed at orbital altitude assuming that the truth model is EGM96, $n_{\max} = 90$). The following numerical evidence demonstrate the effectiveness and efficiency of our algorithm.

First of all we illustrate the convergence of the minimal energy interpolating spline to some given test functions:

$$\begin{aligned} f_1(x, y, z) &= r^{-9} \sin^8(\theta) \cos(8\phi), \\ f_2(x, y, z) &= r^{-11} \sin^{10}(\theta) \sin(10\phi), \\ f_3(x, y, z) &= r^{-16} \sin^{15}(\theta) \sin(15\phi), \\ f_4(x, y, z) &= 789/r + f_3(x, y, z), \end{aligned}$$

where $r = \sqrt{x^2 + y^2 + z^2}$. All of them are harmonic. Let $\triangle$ be a triangulation of the unit sphere which consists of 8 congruent spherical triangles obtained by restricting the spherical surface over each octant of the three dimensional coordinate system. We then uniformly refine it several times as described in Sect. 2 to get new triangulations $\triangle_1, \triangle_2, \triangle_3, \ldots$. That is, $\triangle_n$ is the uniform refinement of $\triangle_{n-1}$. Thus, $\triangle_1$ consists of 18 vertices and 32 triangles, $\triangle_2$ contains 66 vertices and 128 triangles, $\triangle_3$ has 258 vertices and 512 triangles, $\triangle_4$ consists of 1,026 vertices and 2,048 triangles and $\triangle_5$ contains 4,098 vertices and 8,172 triangles.

Recall that $S_5^1(\triangle_n)$ is the C^1 quintic spherical spline space over triangulation $\triangle_n$. We choose

$$r = 1.05 \approx \frac{R_e + 450}{R_e},$$

where $R_e = 6,371.388$ km is the radius of the Earth and 450 km represents the CHAMP orbital height above the surface of the Earth.

The minimal energy spline functions in $S_5^1(\triangle_n)$ with $n = 4$ and $n = 5$ interpolates 16,200 points equally spaced grid points over $[-\pi, \pi] \times [0, \pi]$. To compute these spline interpolants, we use the domain decomposition technique.

Journal: 190 MS: 283 CMS: GIVE CMS ☐TYPESET ☐DISK ☐LE ☐CP Disp.:2008/11/10 Pages: 14 Layout: Large

Table 1 Maximum errors of C^1 quintic interpolatory splines for various functions

	Δ_4		Δ_5	
	rms	Maximum errors	rms	Maximum errors
f_1	$5.091e-04$	$1.242e-02$	$6.566e-06$	$1.269e-04$
f_2	$6.959e-04$	$1.715e-02$	$9.556e-06$	$1.827e-04$
f_3	$1.2313 \times e-03$	$3.011e-02$	$2.756e-05$	$3.549e-04$
f_4	$1.213 \times e-03$	$3.010e-02$	$2.753e-05$	$3.549e-04$

The following numerical results are based on the domain decomposition technique with $q = 3$ and Ω_i being triangles in $\triangle_n$ as described in Sect. 3.1.

Then we estimate the accuracy of the method by evaluating the spline interpolants and the exact functions over 28,796 points almost evenly distributed over the sphere and then computing the maximum absolute value of the differences and computing the root mean square (rms)

$$\text{rms} = \sqrt{\frac{\sum_{i=1}^{28796}(s(p_i) - f(p_i))^2}{28796}},$$

where s and f stand for spline interpolant and function to be interpolated and p_i stands for points over the surface at the orbital level. The root mean square and maximum errors are listed in Table 1.

From Table 1, we can see that the spherical interpolatory splines approximate these functions very well on the spherical surface with radius $r = 1.05$. This example also shows that our domain decomposition technique works very well. The computing time is 30 min for finding spline interpolants in $S_5^1(\Delta_4)$ and 2 h for $S_5^1(\triangle_5)$ using a SGI computer (Tezro) with four processes with 2G memory each.

Let us make a remark. Although these functions may be approximated by using spherical harmonics better than spherical splines, the main point of the table is to show how well spherical splines can approximate. Intuitively, the geopotential does not behave nicely as these test functions and it is hard to approximate by one spherical harmonic polynomial. Instead, by breaking the spherical surface $\mathbb{S}^2$ into many triangles, triangulated spherical splines, piecewise spherical harmonics may have a hope to approximate the geopotential better.

Next we compute interpolatory splines S_V over the given set of data measurements of the geopotential on the orbital surface. We first compute an minimal energy interpolatory spline using the data locations and values over the 2-day period. The spline space $S_5^1(\triangle_4)$ is used, where triangulation $\triangle_4$ consists of 1,026 points and 2,048 triangles. Although the interpolatory spline fits the first 2 day's measurements (5,760 locations and values) to the accuracy 10^{-6}, the root mean square of the spline over the 30-day measurement values is $0.60\,\text{m}^2/\text{s}^2$.

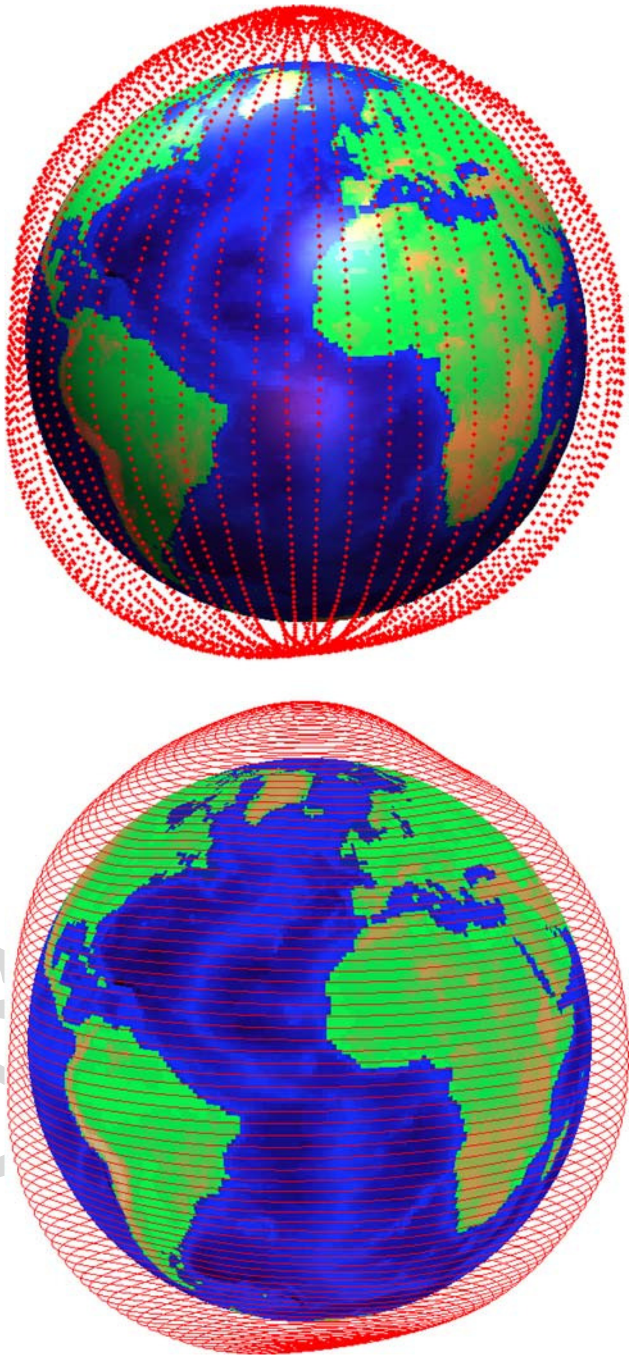

Fig. 4 Normalized geopotential values over the Earth and C^1 quintic spherical spline interpolatory surface

Furthermore we compute the minimal energy interpolatory spline in $S_5^1(\triangle_5)$ which interpolates 23,032 data locations and values over an 8-day period. The root mean square error of the spline at all 86,400 data locations and values of 30 days is $0.018\,\text{m}^2/\text{s}^2$. This shows that the minimal energy spline fits the geopotential over the orbital surface very well. In Fig. 4, we show the geopotential measurements (after a normalization such that the normalized geopotential values

Journal: 190 MS: 283 CMS: GIVE CMS ☐ TYPESET ☐ DISK ☐ LE ☐ CP Disp.:2008/11/10 Pages: 14 Layout: Large

are all bigger than the mean radius of the Earth) and the interpolatory spline surface around the Earth. The normalized geopotential and the spline surface are plotted in 3D view.

4 Approximation of geopotential on the Earth's surface

4.1 The inverse problem

Let S_V be the spherical spline approximation of the geopotential V on the orbit. Recall from the previous section that S_V approximates V very well. We now discuss how we can compute spline approximation s_V of the geopotential V on the Earth's surface.

Let $\triangle_e$ be a triangulation on the unit sphere induced by the triangulation $\triangle$ on the orbital spherical surface used in the previous section. Let $s_V \in S_d^0(\triangle_e)$ be a spline function $s_V = \sum_{T\in\triangle_e}\sum_{i+j+k=d} c_{ijk}^T B_{ijk}^T$ solving the following collocation problem

$$S_V(u) = R_e\frac{|u|^2-R_e^2}{4\pi}\int\limits_{\lambda'=0}^{2\pi}\int\limits_{\theta'=0}^{\pi}\frac{s_V(\theta',\lambda')}{\ell^3}\sin\theta'\mathrm{d}\theta'\mathrm{d}\lambda',$$
$$\text{for } u\in\mathcal{D}_\triangle^d, \tag{4.1}$$

where $\mathcal{D}_\triangle^d$ is the collection of domain points of degree d on $\triangle$, i.e.,

$$\mathcal{D}_\triangle^d := \{\xi_{lmn} = \frac{lv_1+mv_2+nv_3}{\|lv_1+mv_2+nv_3\|_2},$$
$$T=\langle v_1,v_2,v_3\rangle\in\triangle, l+m+n=d\}.$$

More precisely, Eq. (4.1) can be written as follows: Find coefficients c_{ijk}^T such that

$$\sum_{T\in\triangle}\sum_{i+j+k=d} c_{ijk}^T R_e\frac{|u|^2-R_e^2}{4\pi}\int\limits_T\frac{B_{ijk}^T(\theta',\lambda')}{\ell^3}$$
$$\times\sin\theta'\mathrm{d}\theta'\mathrm{d}\lambda' = S_V(u),\quad u\in\mathcal{D}_\triangle^d. \tag{4.2}$$

Note that we use continuous spherical spline space $S_d^0(\triangle_e)$ since the geopotential is not very smooth on the surface of the Earth.

We need to show that the collocation problem (4.1) above has a unique solution as well as s_V is a good approximation of V on the Earth's surface. To this end, we begin with the following

Lemma 4.1 *Let f be a function in $L_2(\mathbb{S}^2)$. Define*

$$F(|u|,\theta,\phi) = \frac{|u|^2-1}{4\pi}\int\limits_{\theta'=0}^{2\pi}\int\limits_{\phi'=0}^{\pi}\frac{f(\theta',\phi')}{\ell^3}\sin\theta'\mathrm{d}\theta'\mathrm{d}\phi',$$
$$\forall\theta,\phi. \tag{4.3}$$

Suppose that for all $|u|=R>1$, $F(u)=0$. Then $f=0$.

Proof It is clear that F is a harmonic function which decays to zero at ∞. We can express F in an expansion of spherical harmonic functions as in (1.1) and (1.2). Now $F(u)\equiv 0$ implies that the coefficients in the expansion have to be zero. That is, by using (1.2),

$$\frac{2n+1}{4\pi}\int\limits_{\theta'=0}^{2\pi}\int\limits_{\phi'=0}^{\pi} f(\theta',\phi')P_n(\cos\psi)\sin\theta'\mathrm{d}\theta'\mathrm{d}\phi' = 0,$$
$$\forall n\geq 0.$$

Thus, $f\equiv 0$. This completes the proof. □

This is just say that if a solution of the exterior Poisson equation is zero over whole layer $|u|=R_0$, it is a zero harmonic function.

Theorem 4.2 *There exists a triangulation $\triangle_e$ such that the minimization (4.1) has a unique solution.*

Proof If the minimization (4.1) has more than one solution, then the observation matrix associated with (4.1) is singular. Thus there exists a spline $s_0\in S_d^r(\triangle_e)$ such that

$$\int\limits_{\theta'=0}^{2\pi}\int\limits_{\phi'=0}^{\pi}\frac{s_0(\theta',\phi')}{\ell^3}\sin\theta'\mathrm{d}\theta'\mathrm{d}\phi' = 0, \tag{4.4}$$

for all θ,ϕ which are associated with the domain points $\mathcal{D}_\triangle^d$ of degree d. That is, the points $u\in\mathbf{R}^3$ with length R_o and angle coordinates (θ,ϕ) are domain points in $\mathcal{D}_{\triangle_1}^d$. Without loss of generality, we may assume that $\|s_0\|_2=1$. Let us refine $\triangle$ uniformly to get $\triangle_1$. Write $\triangle_{e,1}$ to be the triangulation induced by $\triangle_1$. If the linear system in (4.1) replacing $\triangle$ by $\triangle_1$ is not invertible, there exists a spline $s_1\in S_d^0(\triangle_{e,1})$ such that $\|s_1\|_2=1$ and

$$\int\limits_{\theta'=0}^{2\pi}\int\limits_{\phi'=0}^{\pi}\frac{s_1(\theta',\phi')}{\ell^3}\sin\theta'\mathrm{d}\theta'\mathrm{d}\phi', \tag{4.5}$$

for those angle coordinates (θ,ϕ) such that vectors $u\in\mathbf{R}^3$ with length R_o and angle coordinates (θ,ϕ) are domain points in $\mathcal{D}_{\triangle_1}^d$.

In general, we would have a bounded sequence $s_0, s_1, \ldots,$ in $L_2(R_e\mathbb{S}^2)$. It follows that there exists a subsequence $s_{n'}$ which converges weakly to a function $s_*\in L_2(R_e\mathbb{S}^2)$. Then

$$0=\int\limits_{\theta'=0}^{2\pi}\int\limits_{\phi'=0}^{\pi}\frac{s_*(\theta',\phi')}{\ell^3}\sin\theta'\mathrm{d}\theta'\mathrm{d}\phi',\quad\forall(\theta,\phi). \tag{4.6}$$

By Lemma 4.1, we would have $s_*\equiv 0$ which contradicts to $\|s_*\|_2=1$. This completes the proof. □

Journal: 190 MS: 283 CMS: GIVE CMS ☐ TYPESET ☐ DISK ☐ LE ☐ CP Disp.:2008/11/10 Pages: 14 Layout: Large

Using the above Theorem 4.2, we can compute a spline approximation s_V of V over certain triangulations. Next we need to show s_V is a good approximation of V on the Earth's surface. Recall $R_o = R_e + 450\,\text{km}$ with R_e being the mean radius of the Earth. Let

$$\widetilde{V}(R_o, \theta, \phi)$$

$$= R_e \frac{R_o^2 - R_e^2}{4\pi} \int_{\theta'=0}^{2\pi} \int_{\phi'=0}^{\pi} \frac{s_V(\theta', \phi')}{\ell^3} \sin\theta' d\theta' d\phi', \quad (4.7)$$

for all (θ, ϕ). In particular, $\widetilde{V}(R_o, \theta, \phi)$ agrees $S_V(\theta, \phi)$ for those angle coordinates (θ, ϕ) that their associated vectors $u \in \mathcal{D}^d_\triangle$ by Eq. 4.1. That is, S_V is also an interpolation of $\widetilde{V}$. Thus S_V is a good approximation of $\widetilde{V}$ by Lemma 4.3 to be discussed later and thus,

$$\|V - \widetilde{V}\|_{\infty, R_o\mathbb{S}^2} \leq \|V - S_V\|_{\infty, R_o\mathbb{S}^2} + \|S_V - \widetilde{V}\|_{\infty, R_o\mathbb{S}^2}$$

is very small, where the maximum norm $\|\cdot\|_{\infty, R_o}$ is taken over the surface of the sphere with radius R_o.

In addition, we shall prove that

$$\|V - s_V\|_{\infty, R_e\mathbb{S}^2} \leq C\|V - \widetilde{V}\|_{\infty, R_o\mathbb{S}^2}. \quad (4.8)$$

by using the open mapping theorem (cf. Rudin 1967). Indeed, define a smooth function

$$L(f)(\theta, \phi) := R_e \frac{R_o^2 - R_e^2}{4\pi} \int_{\theta'=0}^{2\pi} \int_{\phi'=0}^{\pi} \frac{f(R_e, \theta', \phi')}{\ell^3}$$

$$\times \sin\theta' d\theta' d\phi' \quad (4.9)$$

for all (θ, ϕ). Let $H = \{L(f)(\theta, \phi),\ f \in L_2(R_e\mathbb{S}^2)\}$, where $L_2(R_e\mathbb{S}^2)$ is the space of all square integrable functions on the surface of the sphere $R_e\mathbb{S}^2$. It is clear that H be a linear vector space. If we equip H with the maximum norm, H is a Banach space.

Then $L(f)$ is a bounded linear map from $L_2(R_e\mathbb{S}^2)$ to H which is 1 to 1 by Lemma 4.1. Since L is also an onto map from $L_2(R_e\mathbb{S}^2)$ to H. By the open mapping theorem (cf. Rudin 1967), L has a bounded inverse. Thus, we have Eq. (4.8). We remark that this is different from the integral operator. Indeed, our S_V at the orbital surface and s_V at the surface of the Earth have no radial part. They are just defined on the subdomain with $|u| = R_o$ and $|u| = R_e$ respectively. That is, from S_V we can not downward continuation to get s_V at $r = R_e$ or $R_e/r = 1$. We have to solve (4.1) in order to get the approximation on the surface of the Earth. Certainly, the constant for the boundedness in the discussion above may be dependent on 450 km.

By Theorem 3.4, we have

$$\|V - S_V\|_{\infty, R_o\mathbb{S}^2} \leq C|\triangle|^2,$$

where $|\triangle|$ denotes the size of triangulation $\triangle$. Thus we only need to estimate $\|S_V - \widetilde{V}\|_{\infty, R_o\mathbb{S}^2}$. To this end, we first note that $\widetilde{V}(u) = S_V(u)$ for $u \in \mathcal{D}^d_\triangle$. The following Lemma (see Baramidze and Lai 2005 for a proof) ensures the good approximation property of S_V to $\widetilde{V}$.

Lemma 4.3 *Let T be a spherical triangle such that $|T| \leq 1$ and suppose $f \in W^{2,p}(T)$ vanishes at the vertices of T, that is $f(v_i) = 0$, $i = 1, 2, 3$. Then for all $v \in T$,*

$$|f(v)| \leq C \tan^2\left(\frac{|T|}{2}\right) |f|_{2,\infty,T} \quad (4.10)$$

for some positive constant C independent of f and T.

It follows that

$$|S_V(u) - \widetilde{V}(u)| \leq C \tan^2\left(\frac{|\triangle|}{2}\right) (\|S_V\|_{2,\infty,R_o\mathbb{S}^2}$$

$$+ \|\widetilde{V}\|_{2,\infty,R_o\mathbb{S}^2}).$$

Recall that $\|S_V\|_{2,\infty,R_o\mathbb{S}^2} \leq C\|V\|_{2,\infty,R_o\mathbb{S}^2}$ and $\|\widetilde{V}\|_{2,\infty,R_o\mathbb{S}^2} \leq C\|S_V\|_{2,\infty,R_o\mathbb{S}^2}$. Therefore we conclude the following

Theorem 4.4 *There exists a spherical triangulation $\triangle$ of the surface of the sphere $R_e\mathbb{S}^2$ such that the solution s_V of the linear system (4.1) approximates the geopotential V on the surface of Earth in the following sense*

$$\|s_V - V\|_{\infty, R_e\mathbb{S}^2} \leq C|\triangle|^2 \quad (4.11)$$

for a constant C dependent on the geopotential V on the orbital surface.

4.2 A computational method for the solution of the inverse problem

Finally we discuss the numerical solution of the linear system (4.1). Clearly, when the number of data locations increases, so is the size of linear system. It is expensive to solve such a large linear and dense system. Let us describe the multiple star technique as follows. For each triangle $T \in \triangle_e$, let $\text{star}^\ell(T)$ be the ℓ-star of triangle T. We solve c^T_{ijk}, $i + j + k = d$ by considering the sublinear system which involves all those coefficients c^t_{ijk}, $i + j + k = d$ and $t \in \text{star}^\ell(T)$ for a fixed $\ell > 1$ using the domain points $u \in \text{star}^\ell(T)$. That is, we solve

$$\sum_{t \in \text{star}^\ell(T)} \sum_{i+j+k=d} \widetilde{c}^t_{ijk} R_e \frac{|u|^2 - R_e^2}{4\pi}$$

$$\times \int_t \frac{B^t_{ijk}(v)}{|u - R_e v|^3} d\sigma(v) = S_V(u), \quad (4.12)$$

for $u \in \mathcal{D}^d_\triangle \cap \text{star}^\ell(T)$. We solve (4.12) for each $T \in \triangle_e$. Clearly this can be done in parallel. Let us now show that the solution from the multiple star technique converges to the original solution as ℓ increases. To explain the ideas, we express the system in the standard format:

$$Ax = b$$

Journal: 190 MS: 283 CMS: GIVE CMS ☐ TYPESET ☐ DISK ☐ LE ☐ CP Disp.:2008/11/10 Pages: 14 Layout: Large

with $A = (a_{ij})_{1\le i,j\le n}, x = (x_1,\ldots,x_n)^T$ and $b = (b_1,\ldots,b_n)^T$. Note that entries a_{ij} have the following property:

$$a_{ij} = O\left(\frac{1}{|i-j|^3+1}\right)$$

since coefficients in (4.2) is $\int_T \frac{B^T_{ijk}}{|u-v|^3} d\sigma(v)$ for some triangle T and (i,j,k) with $i+j+k = d$. For domain points u on $\triangle$ of degree d, the distance $|u-v|$ is increasing when u locates far away from $v \in T$. Our numerical solution (4.12) can be expressed simply by

$$\sum_{|i-i_0|\le N_\ell} a_{ij}\tilde{x}_i = b_j, \quad |j-i_0| \le N_\ell$$

for $i_0 = 1,\ldots,n$, where N_ℓ is an integer dependent on ℓ. If ℓ increases, so does N_ℓ. We need to show that $\tilde{x}_i$ converges to x_i as ℓ increases. To this end, we assume that $\|x\|_\infty$ is bounded and the submatrices

$$[a_{ij}]_{|i-i_0|\le N_\ell, |j-j_0|\le N_\ell}$$

have uniform bounded inverses for all i_0. Letting $e_i = x_i - \tilde{x}_i$,

$$\sum_{|i-i_0|\le N_\ell} a_{ij}e_i = -\sum_{|i-i_0|>N_\ell} a_{ij}x_i, \quad |j-i_0| \le N_\ell.$$

Then the terms in the right-hand side can be bounded by

$$\left|\sum_{|i-i_0|>N_\ell} a_{ij}x_i\right| \le C\sum_{j=N_\ell+1}^{\infty}\frac{1}{1+|j|^3} \le C\frac{1}{1+N_\ell^2}$$

and hence,

$$|e_i| \le MC\frac{1}{1+N_\ell^2}$$

for all i. The above discussions lead to the following

Theorem 4.5 *Let $\tilde{c}^T_{ijk}$ be the solution in (4.12) using the multiple star technique. Then $\tilde{c}^T_{ijk}$ converge to c^T_{ijk} as the number ℓ of the star$^\ell(T)$ increases.*

4.3 Computational results on the Earth's surface

In this subsection we use spherical splines to solve the inverse problem as described in Sect. 4. We first wrote a FORTRAN program to solve Eq. (4.2) directly. We tested our program for the following spherical harmonic functions

$$f_1(x,y,z) = \sin^8(\theta)\cos(8\phi),$$
$$f_2(x,y,z) = \sin^{15}(\theta)\sin(15\phi),$$
$$f_3(x,y,z) = 789 + \sin^{15}(\theta)\sin(15\phi)$$

in spherical coordinates. Clearly, $F_1(x,y,z) = r^{-9}f_1(x,y,z)$, $F_2(x,y,z) = r^{-16}f_2(x,y,z)$, and $F_3(x,y,z) = 789/r + r^{-16}f_2(x,y,z)$ are natural homogeneous extension of f_1, f_2, and f_3, where $r^2 = x^2+y^2+z^2$. We use the

Table 2 Maximum errors of C^1 cubic splines over various triangulations

	Δ_0	Δ_1	Δ_2
f_1	0.35138	0.06905	0.003720
f_2	1.36733	0.22782	0.049460
f_3	2.13489	0.81975	0.165639

Table 3 Maximum errors of C^1 quartic splines over various triangulations

	Δ_0	Δ_1	Δ_2
f_1	$3.3684e-01$	$4.63305e-02$	$3.72039e-03$
f_2	1.423358	$1.2708e-01$	$1.4788e-02$
f_3	1.49262	0.41301	0.11598

Table 4 Maximum errors of C^1 quintic splines over various triangulations

	Δ_0	Δ_1	Δ_2
f_1	$1.5857e-01$	$1.2766e-02$	$9.19161e-04$
f_2	$4.5208e-01$	$2.9861e-02$	$2.3973e-03$
f_3	1.99722	0.18698	0.10227

triangulations Δ_n over the unit sphere as explained in the previous section and spherical spline spaces $S^1_d(\Delta_n)$ and $n = 0, 1, 2$ and $d = 3, 4, 5$. Suppose that the function values of F_i at $r = 1.05$ with domain points of Δ_n are given. We compute the spline approximation s_i on the surface of the sphere by

$$F_i(u) = \frac{1}{4\pi}\int_{\mathbb{S}}\frac{s_i(v)}{|u-v|^3}d\sigma(v),$$

where $u = 1.05(\cos\theta\sin\phi, \sin\theta\sin\phi, \cos\phi)$ for (θ,ϕ) as we explained in Sect. 4. We then evaluate s_i at 5,760 points almost evenly distributed over the sphere and compare them with the function values of f_i at these points. The maximum errors are given in Tables 2, 3, and 4 for $d = 3, 4, 5$. From these tables we can see that the numerical values from our program approximate these standard spherical harmonic polynomials pretty well.

We are not able to compute the approximation over refined triangulations Δ_n with $n = 4$ and 5 since the linear system is too large for our computer when we solve (4.2) directly. Thus we have to implement the multiple star method described in Sect. 4.2. That is, we implemented (4.12) in FORTRAN and we can solve (4.12) for each triangle T. Let us explain our implementation a little bit more. To make each submatrix associated with a triangle is invertible for any triangulation, we actually used a least squares technique. That is, we solves

$$A^TAx = A^Tb,$$

Table 5 Errors of C^0 cubic splines over T_{158}

	$\ell = 4$	$\ell = 5$	$\ell = 6$
f_1(maximum errors)	0.0270	0.00587	0.01018
f_2(maximum errors)	0.0429	0.0388	0.0367
f_3(maximum errors)	65.19	20.31	16.04
f_3(relative errors)	8.26%	2.57%	2.03%

Table 6 Errors of C^0 cubic splines over T_{209}

	$\ell = 4$	$\ell = 5$	$\ell = 6$
f_1(maximum errors)	0.0892	0.0403	0.0114
f_2(maximum errors)	0.0594	0.0633	0.0669
f_3(maximum errors)	247.9	56.66	37.68
f_3(relative errors)	31.4%	7.18%	4.77%

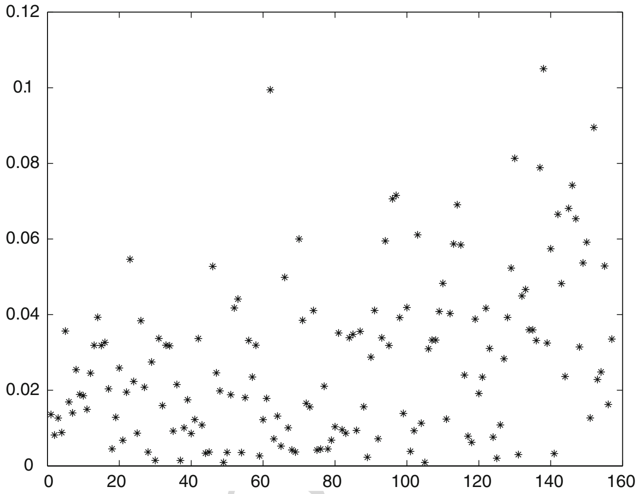

Fig. 5 Values of relative errors

with rectangular matrix A. In fact we choose more domain points in each triangle than the domain points of degree d. Our discussion of the multiple star method in Sect. 4 can be applied to this new linear system. That is, Theorem 4.5 holds for this situation.

In the following we report the numerical experiments based on the multiple star technique for computing the geopotential one triangle at a time. We first present the convergence for the three test functions f_1, f_2, and f_3. We consider $\triangle_3$ with 258 vertices and 512 triangles and choose 5 triangles $T_{65}, T_{158}, T_{209}, T_{300}, T_{400}$. We use C^0 cubic spline functions and ring number $\ell = 4, 5, 6$. By feeding $F_i(x, y, z)$ with $r = 1.05$ into the FORTRAN program we compute spline approximation s_i of f_i at $r = 1$. In Table 5 we list the maximum errors and maximal relative errors which are computed based on 66 almost equally spaced points over triangle T_{158}.

Similarly, we list the maximal absolute errors and maximal relative errors over triangle T_{209} in Table 6. The maximal absolute and relative errors are computed based on 66 almost equally spaced points over triangle T_{209}.

The maximal absolute and relative errors over other T_{65}, T_{300}, T_{400} have the similar behaviors. We omit them to save space here.

Next we compute the geopotential on the Earth's surface using the simulated in situ geopotential measurements generated for the gravity mission satellite, CHAMP (cf. Reigber et al. 2004). In order to check the accuracy of our numerical solution, we compare it with the solution obtained from the traditional spherical harmonic series with degree 90. We used the CHAMP data (from EGM96 model with $1\,\mathrm{m}^2/\mathrm{s}^2$ random noises) at a fixed satellite orbit 450 km above the mean equatorial radius of the Earth. Using the traditional spherical harmonic series with radius $R_e/r = 1$, we compute the geopotential at the Earth's surface at (θ_i, ϕ_j) with $\theta_i = -89° + 2°(i-1)$, $i = 1, \ldots, 90$ and $\phi_j = -180° + 2°(j-1)$, $j = 1, 2, \ldots, 180$ which we refer as the "exact" solution.

We first use our FORTRAN program to compute a spline approximation based on the given measurements from the CHAMP (in the model EGM'96 with $1\,\mathrm{m}^2/\mathrm{s}^2$ noises) and compute a spline solution at the surface of the Earth (the surface of the mean radius of the Earth) to compare with the "exact" solution. We compute the spline solution restricted to 8 triangles $T_{65}, T_{156}, T_{158}, T_{159}, T_{160}, T_{209}, T_{300}, T_{400}$. We have to use the multiple star method in order to solve the large linear system. Consider the numerical result from $\ell = 6$ as our spline solution of the geopotential at the surface of the Earth.

There are 157 (θ_i, ϕ_j)'s fell in these 8 triangles and the relative errors of spline approximation against the "exact" solution are plotted in Fig. 5. The horizontal axis is for the indices of these 157 (θ_i, ϕ_j)'s and the vertical axis is for the values of the relative errors of the geopotential in $\mathrm{m}^2/\mathrm{s}^2$. We can see that most of these relative errors are within 5%.

Let us take a closer look at triangle T_{158}. By using standard statistical arguments (cf. Mendenhall and Sincich 2003) we justify how good our spline method is. There are 19 of these (θ_j, ϕ_j)'s fell in T_{158}. The root mean square error s of the spline approximation against the "exact" solution is

$$s = \sqrt{\frac{1}{19}\sum_{i=1}^{19}(y_i - \hat{y}_i)^2} = 6.288,$$

where y_i and $\hat{y}_i$ stand for the exact values and spline values of the geopotential at those locations (θ_m, ϕ_n) which are in T_{158}. The maximum of the relative errors is

$$\max_{i=1,\ldots,19} \frac{|y_i - \hat{y}_i|}{|y_i|} = 3.84\%.$$

Journal: 190 MS: 283 CMS: GIVE CMS ☐ TYPESET ☐ DISK ☐ LE ☐ CP Disp.:2008/11/10 Pages: 14 Layout: Large

The coefficients of determination R^2 (cf. Mendenhall and Sincich 2003, p. 124) is

$$R^2 = 1 - \frac{\mathrm{SSE}}{\mathrm{SS}_{yy}} = \frac{\sum_{i=1}^{19}(\hat{y}_i - \bar{y})^2}{\sum_{i=1}^{19}(y_i - \bar{y})^2} = 98.1\%,$$

where $\bar{y}$ is the mean of the exact values. That is, 98.1% of the sample variation is explained by the spline model. In addition, we also find out that 63.16% of the "exact" values y_i lie within one s of their respective spline predicted values $\hat{y}_i$ and 100% of the "exact" values of y_i are within two s of their respective spline predicted values $\hat{y}_i$. These indicate that the errors are normally distributed. The coefficient of variation(CV), the ratio of the root mean square error s to the mean $\bar{y}$ is 1.79%. This shows that the coefficient of variation is very small and hence, the spline values lead to accurate prediction. Thus the spline method is reasonably accurate for prediction of the geopotential values at other locations within the triangle. Similar for the other triangles.

It should be noted that the "truth" solution is directly computed from spherical harmonic coefficients (EGM96) at the Earth's surface. A more fair comparison would have been generating the "truth" solution using a regional downward continuation from orbital altitude (e.g., using Poisson integrals), to compare with the spline regional solutions. The comparisons done here is for convenience and proof of concept of the proposed alternate gravity field inversion numerical methodology.

5 Conclusion

In this paper we proposed to use triangular spherical splines to approximate the geopotential on the Earth's surface to assess its feasibility as an alternate method for regional gravity field inversion using data from satellite gravimetry measurements. A domain decomposition technique and a multiple star technique are proposed to realize the computational schemes for approximating the geopotential. In particular, our computational algorithms are parallalizable and hence enables us to model regional gravity field solutions over the triangular regions of interest. Thus our algorithms are efficient. The computational results show that triangular spherical splines for the geopotential over the orbital surface at the height of a satellite is reasonable accuracy. The computational results for the geopotential at the Earth's surface are effective in approximation the "exact" geopotential over some triangles. These computational algorithms can be adapted to model the gravity field using GRACE and GOCE measurements (e.g., disturbance potential and gravity gradient measurements at orbital altitude, respectively). However, over other triangles, the approximation are relatively worse, indicating our comparison studies may not be fair to the spline technique and that further improvement in both the theory and numerical computation is warranted.

Acknowledgments The authors want to thank Ms. Jin Xie and Dr. S.C. Han, at the Ohio State University for their assistance on numerical computations and advice, and Dr. Lingyun Ma for her help performing many numerical experiments at the University of Georgia. This study is supported by National Science Foundation's Collaboration in Mathematical Geosciences (CMG) Program. The authors would also like to thanks two anonymous referees and the Editor, Dr. Willi Freeden for their constructive comments and suggestions, which have improved the paper.

References

Alfeld P, Neamtu M, Schumaker LL (1996a) Bernstein-Bézier polynomials on spheres and sphere-like surfaces. Comp Aided Geom Des 13:333–349

Alfeld P, Neamtu M, Schumaker LL (1996b) Fitting scattered data on sphere-like surfaces using spherical splines. J Comp Appl Math 73:5–43

Alfeld P, Neamtu M, Schumaker LL (1996c) Dimension and local bases of homogeneous spline spaces. SIAM J Math Anal 27:1482–1501

Awanou G, Lai MJ (2005) On convergence rate of the augmented Lagrangian algorithms for nonsymmetric saddle point problems. Appl Numer Anal 54:122–134

Baramidze V (2005) Spherical splines for scatterd data fitting. Ph.D. Dissertation, University of Georgia, Athens, GA, USA

Baramidze V, Lai MJ (2005) Error bounds for minimal energy interpolatory spherical splines, Approximation Theory XI. Nashboro Press, Brentwood, pp 25–50

Baramidze V, Lai MJ, Shum CK (2006) Spherical splines for data interpolatory and fitting. SIAM J Sci Comput 28:241–259

Chambodut A, Panet I, Mandea M, Diament M, Holschneider M, Jamet O (2005) Wavelet frames: an alternative to spherical harmonic representation of potential fields. Geophys J Int 163: 875–899. doi: 10.1111/j.1365-246X.2005.02754.x

Fasshauer G, Schumaker LL (1998) Scattered data fitting on the sphere. In: Daehlen M, Lyche T, Schumaker LL (eds) Mathematical methods for curves and surfaces II. Vanderbilt University Press, Nashville, pp 117–166

Fengler MJ, Freeden W, Kohlhaas A, Michel V, Peters T (2007) Wavelet modeling of regional and temporal variations of the Earth's gravitational potential observed by GRACE. J Geodesy 81:5–15

Forsberg R, Sideris M, Shum C (2005) The gravity field and IGGOS. J Geodynamics 40(4–5):387–393. doi:10.1016/j.jog.2005.06.014

Freeden W, Schreiner F (1998) An integrated wavelet concept of physical geodesy. J Geodesy 72:259–281

Freeden W, Schreiner M (2005) Spaceborne gravitational field determination by means of locally supported wavelets. J Geodesy 79: 431–446

Freeden W, Gervens T, Schreiner M (1998) Constructive approximation on the sphere, With applications to geomathematics. Oxford University Press, New York

Freeden W, Michel V, Nutz H (2002) Satellite-to-satellite tracking and satellite gravity gradiometry (advanced techniques for high-resolution geopotential field determination). J Eng Math 43:19–56

Freeden W, Maier T, Zimmermann S (2003) A survey on wavelet methods for (geo) applications. Rev Mat Comput 16:277–310

Journal: 190 MS: 283 CMS: GIVE CMS ☐TYPESET ☐DISK ☐LE ☐CP Disp.:2008/11/10 Pages: 14 Layout: Large

Han SC, Jekeli C, Shum CK (2002) Efficient gravity field recovery using in situ disturbing potential observables from CHAMP. Geophy Rev Lett 29:1025

Han SC, Jekeli C, Shum CK (2003) Static and temporal gravity field recovery using GRACE potential difference observables. Adv Geosci 1:19–26

Han S, Shum C, Jekeli C (2006) Precise estimation of in situ geopotential difference from GRACE low–low satellite-to-satellite tracking and accelerometry data. J Geophys Res 111:B04411. doi:10.1029/2005JB003719

Heiskanen W, Moritz H (1967) Physical geodesy. Freeman, San Francisco

Jekeli C (2005) Spline Representations of Functions on a Sphere for Geopotential Modeling, Rep 475. Dept Civil Environ Eng & Geod Sci, Ohio State University, Columbus, Ohio

Lai MJ, Schumaker LL (2007) Spline functions on triangulations. Cambridge University Press, Cambridge

Lai MJ, Schumaker LL (2008) Domain decomposition method for scattered data fitting. SIAM Numer Anal (in press)

Lehmann R, Klees R (1999) Numerical solution of geodetic boundary value problems using a global reference field. J Geodesy 73:543–554

Lemoine F, Pavlis N, Kenyon S, Rapp R, Pavlis E, Chao B (1998) New high-resolution model developed for Earth's gravitational field, EOS Trans. Am Geophy Union 79(9):117–118

Mayer-Gürr T, Ilk KH, Feuchtinger M, Eicker A (2005a) Global and regional gravity field solutions from GRACE observations, CHAMP/GRACE Science Team Meet. 2004. http://www.gfzpotsdam.de/pb1/JCG

Mayer-Gürr T, Ilk KH, Eicker A, Feuchtinger M (2005b) ITG-CHAMP01: a CHAMP gravity field model from short kinematic arcs over a one-year observation period. J Geodesy 78:462–480

Mayer-Gürr T, Eicker A, Ilk KH (2006) Gravity field recovery from GRACE-SST data of short arcs. In: Flury J, Rummel R, Reigber C, Rothacher M, Boedecker G, Schreiber U (eds) Observation of the Earth system from Space. Springer, Berlin, pp 131–148

Mendenhall W, Sincich T (2003) A second course in statistics: regression analysis, 6th edn. Pearson Education, New Jersey

Neamtu M, Schumaker LL (2004) On the approximation order of splines on spherical triangulations. Adv Comp Math 21:3–20

Panet I, Jamet O, Diament M, Chambodut A (2005) Modeling the Earth's gravity field using wavelet frames. In: Jekeli C, Bastos L, Fernandes J (eds) Gravity, Geoid and space missions. Springer, Berlin, pp 48–53

Panet I, Chambodut A, Diament M, Holschneider M, Jamet O (2006) New insights on intraplate volcanism in French Polynesia from wavelet analysis of GRACE, CHAMP, and sea surface data. J Geophys Res 111(B9):B09403. http://dx.doi.org/10.1029/2005JB004141

Reigber C, Jochmann H, Wunsch J, Petrovic S, Schwintzer P, Barthelmes F, Neumayer K, Konig R, Forste C, Balmino G, Biancale R, Lemonie J, Loyer S, Perosanz F (2004) Earth gravity field and seasonal variability from CHAMP. In: Reigber C, Luhr H, Schwintzer P, Wickert J (eds) Earth Observation with CHAMP. Springer, New York

Rowlands DD, Luthcke SB, Klosko SM, Lemoine FGR, Chinn DS, McCarthy JJ, Cox CM, Anderson OB (2005) Resolving mass flux at high spatial and temporal resolution using GRACE intersatellite measurements. Geophys Res Lett 32:L04310. doi:10.1029/2004GL021908

Rummel R et al. (1999) Gravity field and steady-state ocean circulation mission, Earth Explorer Mission Selection Workshop, ESA, Granada, Spain, 12–15 October 1999

Rudin W (1967) Functional analysis. McGraw-Hill, New York

Schmidt M (1999) Approximate solution of normal equations by eigenvalue decomposition. J Geodesy 73:109–117

Schmidt M, Fabert O, Shum CK (2005a) Towards the estimation of amulti-resolution representation of the gravity field based on spherical wavelets. In: Sansó F (ed) A window on the future of geodesy. Springer, Berlin, pp 362–367

Schmidt M, Kusche J, van Loon J, Shum CK, Han SC Fabert O (2005b) Multi-resolution representation of regional gravity data. In: Jekeli C, Bastos L, Fernandes J (eds) Gravity, Geoid and space missions. Springer, Berlin, pp 167–172

Schmidt M, Fabert O, Shum CK (2005c) On the estimation of a multi-resolution representation of the gravity field based on spherical harmonics and wavelets. J Geodynamcs 39:512–526

Schmidt M, Fengler M, Mayer-Gürr T, Eicker A, Kusche J, Sanchez L, Han SC (2007) Regional gravity modeling in terms of spherical base functions. J Geodesy 81:17–38

Schneider F (1996) The solution of linear inverse problems in satellite geodesy by means of spherical spline approximation. J Geodesy 71:2–15

Tapley B, Bettadpur S, Ries J, Thompson P, Watkins M (2004) GRACE measurements of mass variability in the Earth system. Science 305:503–505

Journal: 190 MS: 283 CMS: GIVE CMS TYPESET DISK LE CP Disp.:2008/11/10 Pages: 14 Layout: Large